## Research Article

# Investigating Equations Used to Design a Very Small Normal-Mode Helical Antenna in Free Space

**Dang Tien Dung,[1] Quoc Dinh Nguyen [ID],[1] Do Quoc Trinh,[1] and Yoshihide Yamada[2]**

[1]*Faculty of Radio-Electronics, Le Quy Don Technical University, Hanoi, Vietnam*
[2]*Malaysia-Japan International Institute of Technology, Universiti Teknologi Malaysia, Kuala Lumpur, Malaysia*

Correspondence should be addressed to Quoc Dinh Nguyen; dinhnq@mta.edu.vn

A normal-mode helical antenna (NMHA) has been applied in some small devices such as tire pressure monitoring systems (TPMS) and radio frequency identification (RFID) tags. Previously, electrical characteristics of NMHA were obtained through electromagnetic simulations. In practical design of NMHA, equational expressions for the main electrical characteristics are more convenient. Electrical performances of NMHA can be expressed by a combination of a short dipole and small loops. Applicability of equations for a short dipole and a small loop to very small normal-mode helical antennas such as antennas around 1/100 wavelengths was not clear. In this paper, accuracies of equations for input resistances, antenna efficiency, and axial ratios are verified by comparisons with electromagnetic simulation results by FEKO software at 402 MHz. In addition, the structure of the antenna equal to $0.021\lambda$ is fabricated, and measurements are performed to confirm the design accuracy.

## 1. Introduction

A compact antenna has been used in some small devices such as tire pressure monitoring systems (TPMS), radio frequency identification (RFID), and some radio devices that require very small sizes [1]. A very small normal-mode helical antenna (NMHA) is the one having good performances with small size. NMHA is equivalent to a combination of an electric dipole and a magnetic dipole. Therefore, NMHA gives designers more freedom to adjust the size for achieving self-resonant structures. Moreover, NMHA can be effectively used in complex environments, including the dielectric and metal environments. Besides that, the NMHA can increase the gain factor when placed on the metal reflecting surface and attached with the tap feed for the impedance matching [2, 3]. Currently, NMHA is being proposed for the usage in medical sensors [4–8].

There are many research results on NMHA; the authors have proposed equations that can be used for designing antennas to achieve self-resonance [9–11], adding the tap

feed to the NMHA for impedance matching [2, 3], calculating stored electromagnetic powers and Q factors of NMHA [12], and applying NMHA in TPMS devices [13, 14] and RFID devices [15].

Previously, electrical characteristics of NMHA were obtained through electromagnetic simulations. In practical design of NMHA, equational expressions for the main electrical characteristics are more convenient. Electrical performances of NMHA can be expressed by a combination of a short dipole and small loops. Applicability of equations for a short dipole and a small loop to very small normal-mode helical antennas such as those around 1/100 wavelengths was not clear. In this paper, accuracies of equational expressions for input resistances, antenna efficiency, and axial ratios are ensured through comparisons with electromagnetic simulation results by FEKO software [16] at 402 MHz. In addition, a $0.021\lambda$ antenna is fabricated, and measurements are performed to confirm the design accuracy. This paper is divided into 5 sections. Section 1 is the introduction. In Section 2, the structure

and characteristic of the very small normal-mode helical antenna are analyzed. Section 3 presents the equations from basic antenna patterns (small loop and small dipole) that can be employed to design NMHA. Section 4 investigates the applicability of equations used to design, and Section 5 is the conclusion.

## 2. Electrical Characteristics of a Normal-Mode Helical Antenna

Figure 1 illustrates the configuration of NMHA [2]. An equivalent current model of NMHA has been given by Kraus [18]. NMHA can be analyzed by the small dipole and the small loop.

A spiral current is divided into a straight current and a loop current, corresponding to an electric current source of a small dipole and a magnetic current source of a small loop. Small dipole and small loop antennas have the input impedance of $R_{rD} - jX_D$ and $R_{rL} + jX_L$, respectively. Here, $R_{rD}$ and $R_{rL}$ express the radiation resistance of the antenna with $R_{rD}$ being the resistance of the small dipole and $R_{rL}$ being the resistance of the small loops, and $R_l$ indicates the dissipated resistance of the antenna wire.

In Figure 1, the antenna length, antenna diameter, and number of turns are denoted by $H_A$, $D_A$, and $N$, respectively; $d$ indicates the diameter of the antenna wire. NMHA can achieve the self-resonance by selecting the sizes of $H_A$, $D_A$, and $N$ carefully.

In the designing and fabricating process, the electrical parameters of NMHA need to be calculated. The basic parameters of NMHA for antenna designing and the method of computing NMHA's parameters are shown in Table 1.

In order to investigate the equations used to design NMHA, we used the FEKO simulator to compare the results of the survey at 402 MHz with the results calculated by using the proposed equation. Simulation parameters of NMHA used in free space are shown in Table 2. The diameter of the antenna wire is set to be $d = 0.5$ mm. Metallic wire is defined as copper with conductivity $\sigma = 58 \times 10^6$ (1/Ωm). Mesh size of the antenna wire is set to be $\lambda/600$. Antenna parameters such as height ($H/\lambda$) and diameter ($D/\lambda$) need to be adjusted to make NMHA achieve the self-resonance in various numbers of turns ($N = 5$, 7, and 10.

## 3. Basic Equations Used to Design NMHA

*3.1. Self-Resonant Structures Based on the Previously Obtained Equation.* From Figure 1, the antenna input impedance is expressed by the following equation:

$$Z_{in} = R_{rD} + R_{rL} + R_l + j(X_L - X_D). \tag{1}$$

The self-resonant condition of NMHA is expressed by $X_L = X_D$. Here, $X_L$ and $X_D$ are the inductive reactance and capacitive reactance of the loop antenna and the dipole
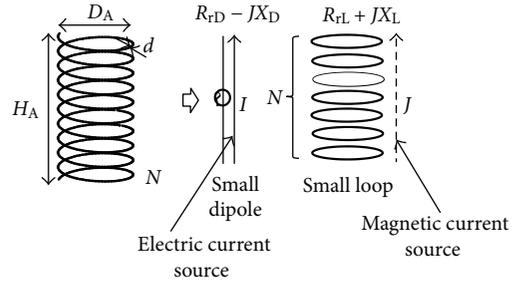


Figure 1: Conceptual equivalence of a normal-mode helical antenna.

Table 1: Parameters for designing NMHA.

| Parameters | Simulator | Equations |
|---|---|---|
| Self-resonant structures ($D_A$, $H_A$, and $N$) | FEKO Software | Suggested [9–11] |
| (i) $R_{rD}$, $R_{rL}$, and $R_l$ | | |
| (ii) Efficiency ($\eta$) | FEKO Software | Not investigated yet |
| (iii) Radiation field ($E_\theta$, $E_\varphi$) | | |
| (iv) Axial ratio (AR) | | |

Table 2: Simulation parameter of NMHA in free space.

| Parameters | Values |
|---|---|
| Frequency | 402 MHz ($\lambda = 745.7$ mm) |
| Mesh size of the antenna wire | $\lambda/600$ |
| Number of turns ($N$) | 5, 7, 10 |
| Diameter of the antenna wire ($d$) | 0.5 mm |
| Metallic wire | Copper ($\sigma = 58 \times 10^6$ (1/Ωm)) |
| Memory | 664 kb |
| Time per each simulation | 5 s |

antenna, respectively. The expressions of $X_L$ and $X_D$ of NMHA depend on antenna structures in free space. These have been given by [9–11] as follows:

$$X_D = \frac{279\lambda H_A}{N\pi(0.92H_A + D_A)^2},$$

$$X_L = \frac{600\pi \times 19.7ND_A^2}{\lambda(9D_A + 20H_A)}. \tag{2}$$

When $X_L = X_D$, from (7) and (8), the self-resonant equation is derived by normalization on both sides of the equation as follows:

$$\frac{279(H_A/\lambda)}{N\pi(0.92(H_A/\lambda) + (D_A/\lambda))^2} = \frac{600\pi \times 19.7N(D_A/\lambda)^2}{9(D_A/\lambda) + 20(H_A/\lambda)}. \tag{3}$$

By solving (3), antenna parameters, including height ($H_A$), diameter ($D_A$), and the number of turns, are determined.

In this paper, only very small NMHA, with the size ranging from $0.005\,\lambda$ to $0.03\,\lambda$, is investigated [9].

The comparison between the result from the simulation and that from (3) was demonstrated in Figure 2. The four structures of NMHA, which were chosen for investigation, are denoted as A, B, C, and D. The structure D is fabricated and measured. Details of these structures are shown in Table 3. A good agreement is obtained between the simulation and the equation results. Therefore, the accuracy of (3) is confirmed.

*3.2. Expressions for Resistances.* NMHA self-resonant structure is achieved when $X_D = X_L$. The input resistance of NMHA is expressed by the following equation:

$$R_A = R_{rD} + R_{rL} + R_l, \tag{4}$$

where the resistance components, the antenna efficiency, and the antenna ratio depend on the structural parameters, which are expressed by [17, 18]

$$R_{rD} = 20\pi^2 \left(\frac{H_A}{\lambda}\right)^2, \tag{5}$$

$$R_{rL} = 320\pi^6 \left(\frac{D_A}{2\lambda}\right)^4 N^2, \tag{6}$$

$$R_l = \alpha \frac{L_t}{d} \sqrt{\frac{120}{\sigma\lambda}}, \tag{7}$$

$$\eta = \frac{R_{rD} + R_{rL}}{R_{rD} + R_{rL} + R_l}, \tag{8}$$

$$\text{AR} = \frac{E_\varphi}{E_\theta}, \tag{9}$$

where $E_\varphi$ is the radiation characteristics of the small loop and $E_\theta$ is the radiation characteristics of the small dipole. Both of them are components in the configurations of NMHA.

# 4. Investigating the Applicability of Equations Used for Defining NMHA Parameters

In order to verify (5), (6), (7), (8), and (9), A, B, C, and D structures in Figure 2 are also investigated. The calculation results are compared with the simulation results by a FEKO simulator.

*4.1. Investigating Equations for Calculating Radiation Resistance.* The radiation resistance of structure A in Figure 2 is as follows: according to (5) and (6), $R_{rD} = 0.177\,\Omega$, $R_{rL} = 0.335\,\Omega$, and the radiation resistance of structure A is $R_r = 0.512\,\Omega$, while the simulation result of the radiation resistance is $R_r = 0.473\,\Omega$. The difference between the simulation and the equation results is $0.039\,\Omega$, corresponding to about 8.2%. Similarly, the radiation resistance obtained at point B is as follows: according to (5) and (6), $R_{rD} = 0.005\,\Omega$, $R_{rL} = 0.035\,\Omega$, and $R_r = 0.040\,\Omega$, while the
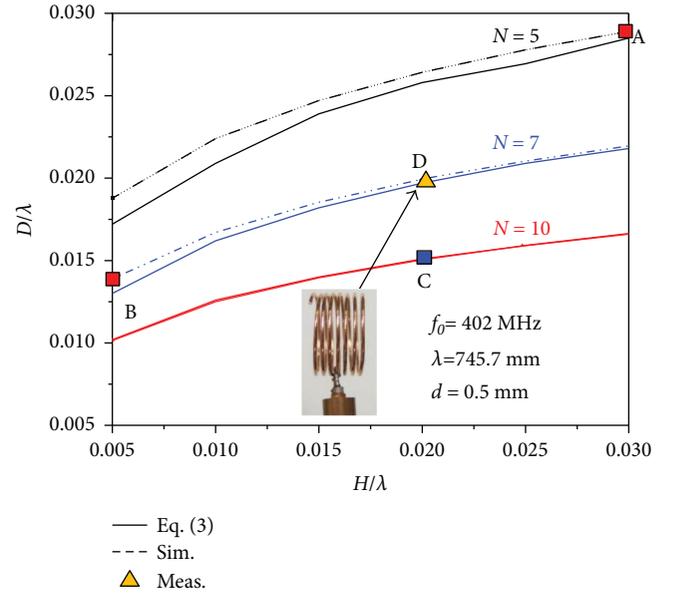


FIGURE 2: Comparing results calculated by equations and the simulation of NMHA self-resonant structure in free space.

TABLE 3: NMHA structures chosen for investigation.

| Values | $H/\lambda$ | | | $D/\lambda$ | | |
|---|---|---|---|---|---|---|
| | Sim. | Eq. | Meas. | Sim. | Eq. | Meas. |
| A ($N = 5$) | 0.03 | 0.03 | | 0.0289 | 0.0285 | |
| B ($N = 7$) | 0.005 | 0.005 | | 0.0138 | 0.0130 | |
| C ($N = 7$) | 0.02 | 0.02 | | 0.0150 | 0.0151 | |
| D ($N = 10$) | 0.021 | 0.021 | 0.021 | 0.0201 | 0.0199 | 0.0195 |

simulation result of radiation resistance is $R_r = 0.031\,\Omega$. The difference between the simulation and the equation results is $0.009\,\Omega$, corresponding to about 29%. Radiation resistance of structure C is obtained as follows: according to (5) and (6), $R_r = 0.178\,\Omega$, while the simulation result of radiation resistance is $R_r = 0.210\,\Omega$. The difference between the simulation and the equation results is $0.032\,\Omega$, corresponding to about 15.2%.

The comparison between the equation results and the simulation results is shown in Figure 3. As can be seen, the simulation and equation results are similar. Because of the very small antenna structure $H_A = 0.005\,\lambda$ ($H_A = 3.729\,\text{mm}$), the radiation resistance becomes very small leading to a difference that is quite large (about 30%). However, this difference is acceptable.

Therefore, (5) and (6) can be used to calculate NMHA resistance radiation with the deviation of less than 30%.

*4.2. Investigating Equations for Calculating Ohmic Resistance.* From (7), $L_t$, $\lambda$, and $\sigma$ are the total length, wavelength, and conductivity, respectively, of the antenna wire. $\alpha$ is the coefficient of the tapered current distribution. $\alpha$ is determined
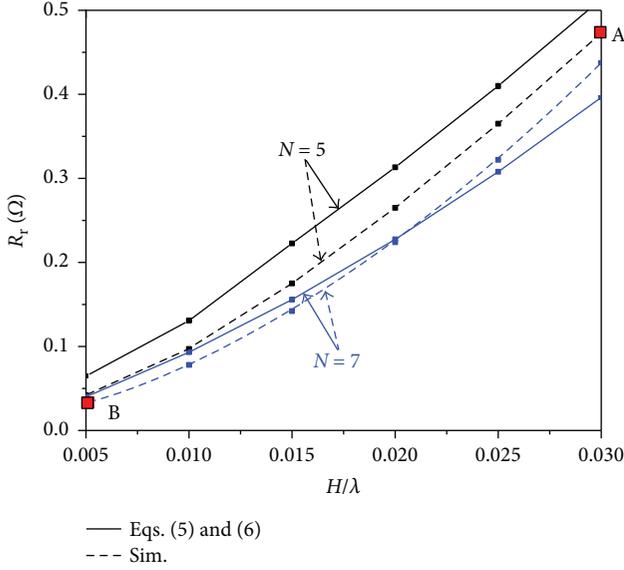
FIGURE 3: Comparison of NMHA radiation resistance in free space between the equation results and the simulation results.



FIGURE 4: Comparison of NMHA ohmic resistance in free space between the equation results and the simulation results.

by calculating the current $I(l)$ along the length of the antenna wire $L_t$ [18].

$$I(l) = I_M \sin \frac{\pi}{L_t} \left( \frac{L_t}{2} - \left| l - \frac{L_t}{2} \right| \right),$$

$$\begin{aligned} I_0 &= \frac{I_M}{L_t} \int_0^{L_t} \sin \frac{\pi}{L_t} \left( \frac{L_t}{2} - \left| l - \frac{L_t}{2} \right| \right) dl \\ &= \frac{I_M}{L_t} \int_0^{L_t/2} \sin \frac{\pi}{L_t} l \, dl + \frac{I_M}{L_t} \int_{\frac{L_t}{2}}^{L_t} \sin \frac{\pi}{L_t} (L_t - l) dl \\ &= \frac{2}{\pi} I_M \cong 0.6 I_M. \end{aligned}$$

$$(10)$$

Here, $I_0$ is the average current of the antenna wire, $I_M$ is the amplitude of the feed current at the middle antenna wire. 0.6 is the appropriate value of $\alpha$. Equation (7) gives the correct results at $\alpha = 0.6$. Figure 4 illustrates the NMHA ohmic resistance in free space. Due to very small structures, $R_l$ is very small. Calculation results by adopting the equation and simulation results are nearly the same.

With structure A, at $N = 5$ and $H_A = 0.03\,\lambda$, the difference of the simulation and the equation results is the largest. The ohmic resistance obtained by (7) equals to $0.676\,\Omega$, and the ohmic resistance obtained by the simulation equals to $0.616\,\Omega$. The difference is $0.06\,\Omega$, corresponding to about 9.8%. Therefore, (7) is relatively accurate; then, it can be used to calculate ohmic resistance with deviation of less than 10%.

When (5), (6), and (7) were investigated, by using (4), the input resistance of NMHA is relatively accurate. Figure 5 illustrates the comparison of NMHA input resistance in free space. It is clear that the simulation and equation results are nearly identical. Therefore, 4 is reliable, with the deviation less than 13%.
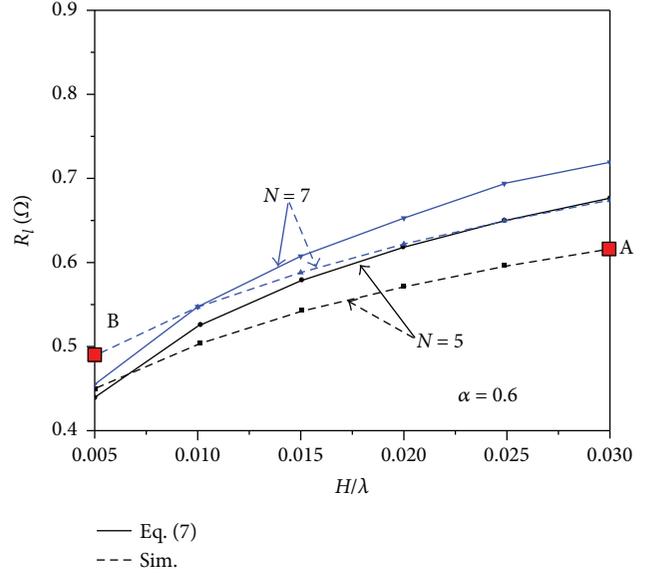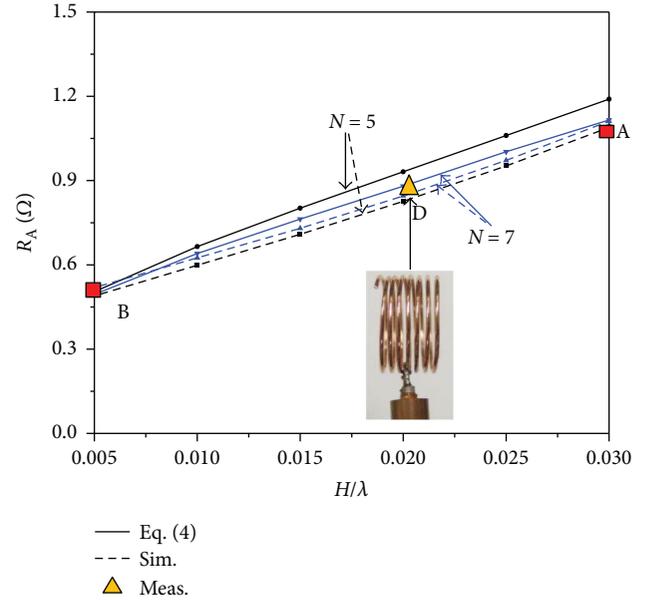


FIGURE 5: Comparisons of NMHA input resistance in free space.

In order to confirm the results of the comparison between (4) and the simulations, the structures of the antenna, which is equal to $0.021\,\lambda$, were fabricated and measured. With structure D, the result of the input resistance ($R_A$) is obtained as follows: the result of the simulation is $0.871\,\Omega$, the result of (4) is $0.961\,\Omega$, and the measured result is $0.888\,\Omega$. The difference between the measurement and the equation results is $0.073\,\Omega$, corresponding to about 8.2%. Hence, (4) is confirmed.

In very small structures, $R_A$ is about $0.5\,\Omega$ to $1.2\,\Omega$, with the NMHA structure being about $0.005\,\lambda$ to $0.03\,\lambda$. Hence,

the radiation resistance is much smaller than that of the transmission line (50 Ω).

### 4.3. Investigating Equations for Calculating Antenna Efficiency.

Figure 6 shows the radiation performance of NMHA obtained by the simulation and (8) in free space. In structure B, the difference between the simulation and equation results is the largest. The antenna efficiency obtained by (8) is equal to 8.07%, and the antenna efficiency obtained by the simulation is equal to 6.20%. It means that the deviation between the antenna efficiency given by the equation and simulation is 1.87%. Among all of the investigated structures, B has the largest deviation (about 30%).

Hence, (8) can be used to calculate NMHA radiation performance in free space with a maximum deviation of 30%. Calculation results also prove that the antenna performance increases when its dimension increases.

The relationship between the antenna structures and antenna efficiency is shown in Figure 7. As observed, NMHA achieves relatively high performance, even its size is very small. When designing NMHA, Figure 7 is the basis to determine the antenna radiation efficiency.

### 4.4. Investigating Equations for Calculating Axial Ratio.

From (9), $E_\theta$ is the radiation characteristics of the small dipole, and it is expressed as

$$E_\theta = \frac{IH_A e^{-JkR}}{J4\pi\omega\varepsilon} \left( \frac{1}{R^3} + \frac{Jk}{R^2} + \frac{k^2}{R} \right) \sin\theta. \quad (11)$$

Here, $I$ indicates the antenna current, $k$ is the wave number, and $R$ is the distance from the antenna. $1/R^3$ and $1/R^2$ represent the static electric field and the inductive electric field, respectively. As the value of $R$ increases, the values of $1/R^2$ and $1/R^3$ decrease rapidly. $1/R$ denotes the far-radiated electric field of the antenna. By applying $\sigma$, $\varepsilon$, and $\omega$ to 11 and then transforming, we obtain the following expression for the radiation characteristics of the small dipole:

$$E_\theta = J \frac{60\pi IH_A \sin\theta}{\lambda R}. \quad (12)$$

From (9), $E_\varphi$ is the radiation characteristics of the small loop, and it is expressed as

$$E_\varphi = -\frac{J\omega\mu INSe^{-jkR}}{4\pi} \left( \frac{1}{R^2} + \frac{jk}{R} \right) \sin\theta. \quad (13)$$

By applying $\sigma$, $\varepsilon$, and $\omega$ to (13) and then transforming, we obtain the following expression for the radiation characteristics of the small loop:

$$E_\varphi = \frac{30\pi^3 IND_A^2 \sin\theta}{\lambda^2 R}. \quad (14)$$

By applying (12) and (14) to (9) and then transforming, we obtain the following expression for the axial ratio as

$$AR = \left| \frac{E_\varphi}{E_\theta} \right| = \frac{\pi^2 ND_A}{2H_A \lambda} = \frac{1}{2}\sqrt{\frac{\pi^4 N^2 D_A^2}{H_A^2 \lambda^2}} = \frac{1}{2}\sqrt{\frac{R_{rL}}{R_{rD}}}. \quad (15)$$
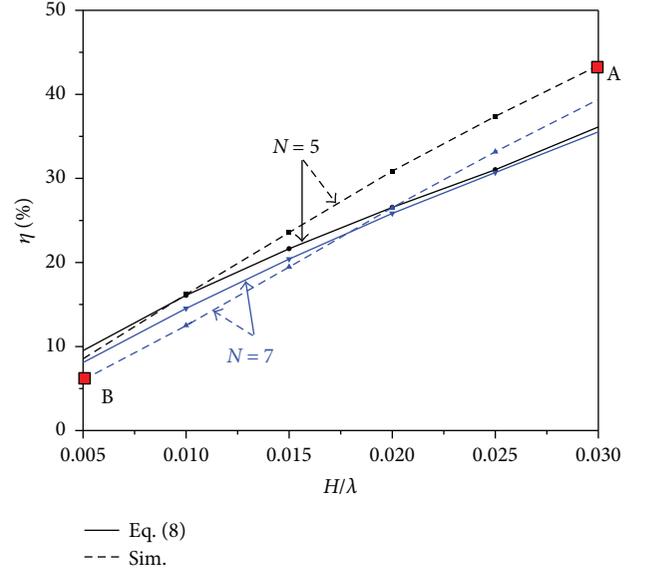


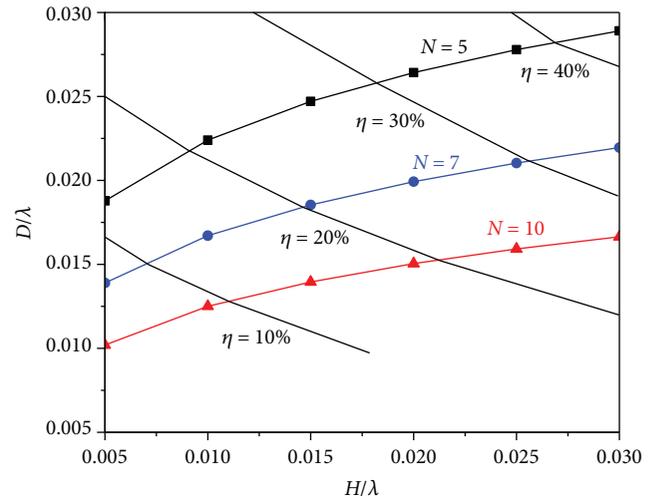FIGURE 6: Comparison of NMHA efficiency.



FIGURE 7: Relationship between the antenna structures and antenna efficiency of NMHA.

Figure 8 shows the calculated results of the axial ratio by using (15) and the simulation. Figure 8 shows that there is a very good agreement between the simulation and equation results, with a maximum deviation of 3%. Therefore, (9) can be used to design NMHA.

The relationship between the antenna structures and axial ratio is displayed in Figure 9. NMHA is possible to adjust its structure for achieving its directivity to meet the application requirements. When AR = 0 dB, the radiation components of the electric dipole and magnetic dipole of NMHA are the same. When AR > 0 dB, the radiation component of the magnetic dipole is larger. When designing NMHA, based on the requirement of using the electric dipole and magnetic dipole, we can use Figure 9 to define the antenna size.
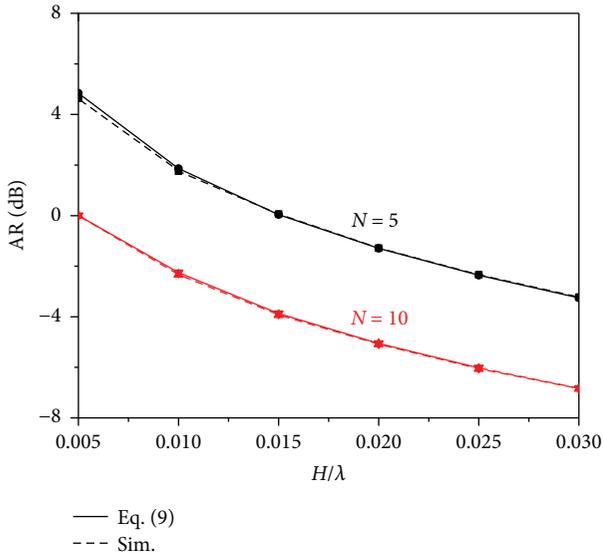
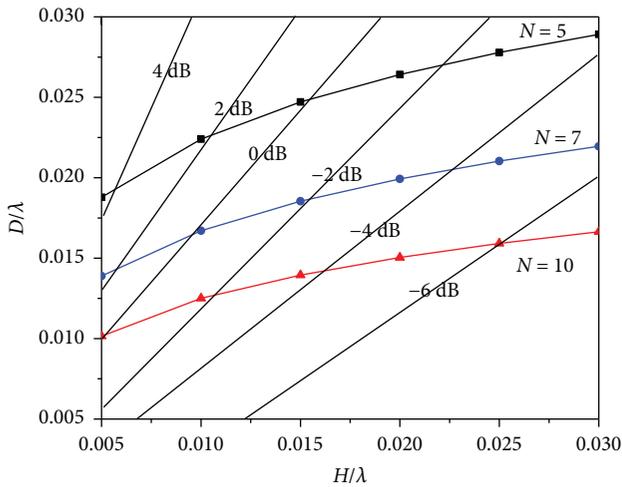FIGURE 8: Comparison of the axial ratio of NMHA.



FIGURE 9: The relationship between the antenna structures and axial ratio.

## 5. Conclusions

In this paper, we investigated the equation use to design very small NMHA (the structure of NMHA is about $0.005\lambda$ to $0.03\lambda$), including self-resonant conditions, radiation resistance, input resistance, antenna efficiency, and axial ratio. The proposed equations at the frequency of 402 MHz are compared to the simulation results performed by a FEKO simulator. The results are as follows: the equation can be used to calculate the radiation resistance with a maximum deviation of 30%. The equation can be used to calculate the ohmic resistance with a maximum deviation of 10%. The equation can be used to calculate the input resistance with a maximum deviation of 13%. The equation can be used to calculate the antenna efficiency with a maximum deviation of 30%. The equation can be used to calculate the axial ratio with a maximum deviation of 3%.

The input resistance results also show that, for very small structures, $R_A$ is very small (about 1 Ω). So, it is necessary to use impedance matching techniques for antennas and transmission lines, although the radiation efficiency is quite large.

In order to improve the calculation of NMHA's parameters, it is necessary to investigate the equations for the purpose of calculating the antenna's bandwidth. This is a problem that will be solved in the future.

## Conflicts of Interest

The authors declare that they have no conflicts of interest.

## References

[1] ASGE, *Wireless Capsule Endoscopy*, American Society for Gastrointestinal Endoscopy, 2013, http://dx.doi.org/10.1016/j.gie.2013.06.026.

[2] N. Q. Dinh, N. Michishita, Y. Yamada, and K. Nakatani, "Design method of a tap feed for a very small normal-mode helical antenna," in *Proceedings of the Asia Pacific Microwave Conference, APMC 2009*, pp. 2416–2419, Singapore, December 2009.

[3] N. Q. Dinh, T. Teranishi, N. Michishita, Y. Yamada, and K. Nakatani, "Simple design equations of tap feeds for a very small normal-mode helical antenna," in *IEEE Antennas and Propagation Society International Symposium*, pp. 1–4, Toronto, ON, Canada, July 2010.

[4] K. Ochiyama, N. Michishita, and Y. Yamada, "Effects of dielectric or magnetic materials to electrical characteristics of very small normal-mode helical antennas," in *IEEE Antennas and Propagation Society International Symposium*, pp. 1-2, Chicago, IL, USA, July 2012.

[5] Australian Communications Authority, *Planning for Medical Implant Communications Systems (MICS) & Related Devices*, 2003.

[6] K. Ochiyama, N. Michishita, and Y. Yamada, "Self resonant structures of very small normal-mode helical antennas in case of containing dielectric or magnetic material inside," in *28th annual review of progress in applied computational Electromagnetics*, pp. 118–121, Columbus, OH, USA, April 2012.

[7] N. T. Tuan, Y. Yamada, D. T. Dung, L. T. K. Bong, N. Q. Dinh, and N. Michishita, "Electrical performances of normal-mode helical antennas used in a human body," in *Vietnam-Japan international symposium on antennas and propagation*, pp. 120–123, Nha Trang, Vietnam, February 2016.

[8] D. T. Dung, N. Q. Dinh, N. T. Tuan, Y. Yamada, and N. Michishita, "Simulation methods of a normal-mode helical antenna in a human body condition," in *International Conference on Advanced Technologies for Communications*, pp. 380–383, Hanoi, Vietnam, October 2016.

[9] N. Q. Dinh, "A design of very small normal mode helical antenna for wireless communication systems," in *2012 International Conference on Advanced Technologies for Communications (ATC)*, pp. 191–194, Hanoi, Vietnam, October 2012.

[10] N. Q. Dinh, N. Michishita, Y. Yamada, and K. Nakatani, "Deterministic equation for self-resonant structures of very small normal-mode helical antennas," *IEICE Transactions on Communications*, vol. E94-B, no. 5, pp. 1276–1279, 2011.

[11] N. Q. Dinh, N. Michishita, Y. Yamada, and K. Nakatani, "Design equation for self resonant structures of very small

normal-mode helical antenna," in *International Symposium on Antennas and Propagation*, pp. 327–330, Macau, China, November 2010.

[12] K. Mouri, N. Michishita, Y. Yamada, and N. Q. Dinh, "Calculation of stored electromagnetic powers and Q factors of very small normal-mode helical antennas," in *International Conference on Advanced Technologies for Communications (ATC)*, Ho Chi Minh City, Vietnam, October 2013.

[13] N. Q. Dinh, T. Teranishi, N. Michishita, Y. Yamada, and K. Nakatani, "FEKO-based method for electromagnetic simulation of carcass wires embedded in vehicle tires," *Applied Computational Electromagnetics Society Journal*, vol. 26, no. 3, pp. 217–224, 2011.

[14] N. Q. Dinh, N. Michishita, Y. Yamada, and K. Nakatani, "Electrical characteristics of a very small normal mode helical antenna mounted on a wheel in the TPMS application," in *2009. APSURSI '09. Antennas and Propagation Society International Symposium*, pp. 1–4, Charleston, SC, USA, June 2009.

[15] W. G. Hong, W. H. Jung, Y. Yamada, and N. Michishita, "High performance normal mode helical antenna for RFID tags," in *2007 IEEE Antennas and Propagation Society International Symposium*, pp. 6023–6026, Honolulu, HI, USA, June 2007.

[16] "EM Software & Systems," FEKO suite 7.0, https://www.feko.info/.

[17] C. A. Balanis, *Antenna Theory, Analysis and Design*, Published simultaneously in Canada, Hoboken, NJ, USA, 3rd edition, 2005.

[18] J. D. Kraus, *Antennas*, McGraw-Hill, New York, NY, USA, 2nd edition, 1988.